International Journal of Thermophysics, Vol. 27, No. 5, September 2006 (© 2006)
DOI: 10.1007/s10765-006-0118-2

Thermal Diffusivity of Metallic Thin Films: Au, Sn, Mo, and Al/Ti Alloy

Sun Rock Choi,[1] Dongsik Kim,[1,2] and Sung-Hoon Choa[3]

Received August 15, 2005

The thermal diffusivity of Au, Sn, Mo, and $Al_{0.97}Ti_{0.03}$ alloy thin films, which are commonly used in microelectromechanical (MEMs) system applications, is measured by two independent methods — the ac calorimetric and photothermal mirage methods. Both methods yield similar results of the thin-film thermal conductivity, but the uncertainty of the mirage technique is found to be relatively large because of the large temperature increase during the measurement. The measured thermal diffusivities of the thin films are generally lower than those of the same bulk material. Especially, the $Al_{0.97}Ti_{0.03}$ thin film shows a pronounced thermal conductivity drop compared with bulk Al, which is believed to be mainly due to impurity scattering. Comparison of the thermal conductivity with the electrical conductivity measured by the standard four-probe technique indicates that the relation of thermal and electrical conductivities follows the Wiedemann–Franz law for the case of Au and Sn thin films. However, the Lorentz number is significantly larger than the theoretical prediction for the case of $Al_{0.97}Ti_{0.03}$ and Mo thin films.

KEY WORDS: ac calorimetric method; AlTi alloy; Au; metal; mirage technique; Mo; Sn; thermal diffusivity; thin film.

1. INTRODUCTION

The thermal diffusivity of a thin film is important in various applications that involve microstructures where thermal energy transport occurs. It has long been recognized that thermal diffusion in thin films may differ significantly from that in the same bulk materials. The transport mechanisms in a thin film are different from those of a bulk material [1], and thus strong

[1] Department of Mechanical Engineering, POSTECH, Pohang 790–784, Korea.
[2] To whom correspondence should be addressed. E-mail: dskim87@postech.ac.kr
[3] MEMS Lab, Samsung Advanced Institute of Technology, Yongin 449–712, Korea.

size dependence is often observed as the film thickness becomes small. Furthermore, the thermal diffusivity of a thin film depends on the microstructure, i.e., fabrication process. Accordingly, it is evident that precise measurement of the thermal diffusivity is a prerequisite for optimal design and analysis of microelectromechanical system (MEMs) devices, particularly, microscale thermal systems.

A number of experimental methods have been suggested for measuring the thermal diffusivity or thermal conductivity of various thin films. In contact methods, including the 3ω method [2] and the micro-sensor method [3], the supplied heat flux and temperature response can be precisely quantified. However, those contact methods require relatively complex sample preparation processes to construct probe metal patterns. An electrical insulation layer has to be added in case the sample is electrically conducting. Therefore, the 3ω method is often limited to dielectric thin films, despite its effectiveness as a standard technique for thermal characterization of a thin film. On the other hand, non-contact methods such as the photothermal technique enable determination of the thermal diffusivity without a special sample-preparation procedure in a non-destructive fashion [4]. However, these non-contact methods require precise alignment of the optical elements used for optical heating and temperature detection. The sensitivity of the non-contact method in detecting the thermal response of the sample is generally worse than that of the contact schemes. As a compromise between contact and non-contact methods, the ac calorimetric method employs non-contact (optical) heating and contact detection of the temperature response [5]. The method is used to measure the thermal diffusivity for a broad range of materials as a result of its simplicity in the experimental setup. However, the sensitivity of the ac calorimetric method strongly depends on the amount of heat flow though the thin film relative to that through the substrate, i.e., $d_f\sqrt{k_f C_f}/d_s\sqrt{k_s C_s}$ where k is the thermal conductivity, C is the heat capacity per unit volume, d is the thickness, and subscripts f and s refer to the film and substrate, respectively. Therefore, either a freestanding structure or a low thermal-conductivity substrate needs to be utilized to ensure good sensitivity in this technique. Using substrates with low thermal conductivity, the thermal diffusivity of submicron films has been measured successfully [5].

In this work, the thermal diffusivities of Au (1000 nm in thickness), Sn (2000 nm), Mo (350 nm), and $Al_{0.97}Ti_{0.03}$ (400 nm) thin films are measured by two independent experimental schemes — the ac calorimetric method and the photothermal mirage technique. Although the metal films are widely used in MEMS applications, their microscale thermal transport characteristics have scarcely been studied. Especially in the case of Sn and $Al_{0.97}Ti_{0.03}$ films, no thermal conductivity data are available in the

open literature. The thermal conductivity of Mo film has been reported for a 100 nm thin film [6]. However, considering the strong size and process dependence of the thin-film thermal diffusivity, it is evident that further investigations are required for Mo as well. For the $Al_{0.97}Ti_{0.03}$ alloy, the addition of Ti is for enhancement of the structural strength of the film. As pointed out earlier, the contact method generally yields more accurate results than such non-contact method as the mirage technique. Nevertheless, the mirage technique is a powerful scheme since it requires no sample preparation process. Therefore, the thermal diffusivity has also been measured by the photothermal mirage technique in separate experiments, in addition to the AC calorimetry measurements. The objective of the additional experiment is mainly to confirm the results of the ac calorimetric method with minimum effort. It is noted that the two methods can share all experimental components except those for temperature detection. Air is used as the coupling fluid in the mirage technique without optimizing the fluid. Accordingly, the mirage scheme that detects the temperature response indirectly through a non-optimized coupling fluid underperforms the ac calorimetric method. Nevertheless, the combined methods are effective for easy verification of the accuracy of the ac calorimetric measurement.

2. THERMAL DIFFUSIVITY MEASUREMENT

Figure 1 displays the principle of the ac calorimetric method for thermal diffusivity determination. When a modulated light source irradiates a part of a thin-film sample, a thermal wave is generated and propagates through the sample. This thermal response is detected by a thermocouple by varying the distance from the heat source. If the sample thickness is

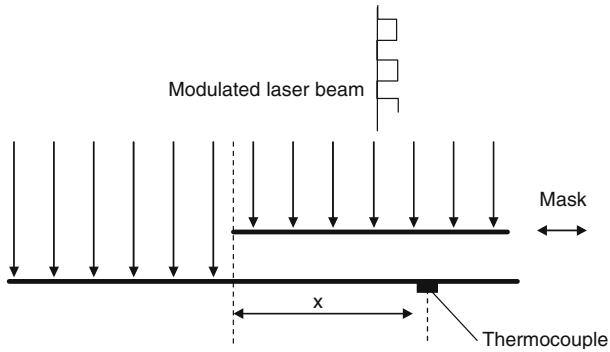

Fig. 1. Principle of the ac calorimetric method.

less than the thermal diffusion length, the temperature is one-dimensional, i.e., uniform in the direction perpendicular to the sample surface. For the case where there is no heat loss from the sample to the ambient air, the temperature oscillation $T(x,t)$ can be expressed as a function of the distance x and time t by

$$T(x,t) = T_0 \exp\left(-x\sqrt{\frac{\omega}{2\alpha}}\right)\cos\left(\omega t - x\sqrt{\frac{\omega}{2\alpha}}\right), \tag{1}$$

where T_0 is a constant determined by the light intensity, α is the thermal diffusivity of the sample, and ω is the angular modulation frequency. According to Eq. (1), the thermal diffusivity of the sample can be measured by analyzing either the amplitude decay or the phase shift of the temperature oscillation by varying the distance x.

If the heat loss from the surface cannot be neglected, the apparent thermal diffusivity α_a determined by the amplitude decay is different from that determined by the phase shift α_p and neither of them gives the correct thermal diffusivity. Gu et al. [7] showed that the thermal diffusivity of the sample in this situation is given by the geometric mean of the two apparent thermal diffusivities, one obtained from the amplitude decay and the other from the phase shift, i.e.,

$$\alpha = \sqrt{\alpha_a \alpha_p}. \tag{2}$$

Therefore, the effect of heat loss can be eliminated by simultaneous measurement of the amplitude decay and the phase lag. Equation (2) overbalances the effect of heat loss only if the heat loss is linearly proportional to the temperature difference between the surface and ambient. The radiation heat loss taking place in the present experiment can be linearized with an error less than 5% since the surface temperature increase is less than 10 K. Consequently, Eq. (2) compensates for the effect of radiation heat loss from the sample surface to the surroundings. When the surface temperature is not small, more rigorous solutions considering the radiation loss should be employed [8].

When the thin-film sample is not freestanding but consists of two layers, the effective thermal diffusivity of the sample is obtained from the properties of each individual layer [5]. Assuming that the total thickness of the sample is less than the thermal diffusion length and the thermal wave propagates only in the direction along the length of the sample, the effective thermal diffusivity of the sample is given by

$$\alpha = \frac{d_f C_f \alpha_f + d_s C_s \alpha_s}{d_f C_f + d_s C_s}, \tag{3}$$

where α_f and α_s represent the thermal diffusivity of the film and the substrate, respectively. Consequently, the thermal diffusivity of the thin film can be determined by Eq. (3).

The theory of thermal diffusivity determination by the photothermal mirage technique is largely similar to that of the ac calorimetric technique, except that a HeNe laser beam replaces the thermocouple and the heat conduction in air should be considered. An analytical solution to the three-dimensional heat conduction problem considering the heat conduction in air as well as in the sample [10] has thus been employed to determine the thermal diffusivity. In this work, a multiparameter fitting scheme has been employed to determine the thermal diffusivity by the mirage technique [9]. Details of the principles of the mirage measurement can be found elsewhere [9–11].

Figure 2 shows the experimental setup for the ac calorimetric method. An argon-ion laser having a wavelength of 488 nm (Spectra-Physics, Model Stabilite 2017) is utilized as a heat source. The output power is modulated by an acousto-optic modulator (AOM, Ismet, Model 1205C-2) at a desired frequency. The frequency is varied in the range from 1 to 10 Hz for the thermal penetration to be greater than the thickness of the samples. The thermal penetration depth $\sqrt{\alpha/\omega}$ is 108 – 342μ m for 1 – 10 Hz. A beam expander enlarges the beam to uniformly cover the entire sample. The frequency of the heating laser beam, is controlled by a function generator and a lock-in amplifier (Stanford Research Systems, Model SR552), detects the signal at the modulated frequency. To probe the temperature oscillation on the sample surface, a K-type thermocouple of 25μm in junction diameter is attached to the lower surface of the sample with a small

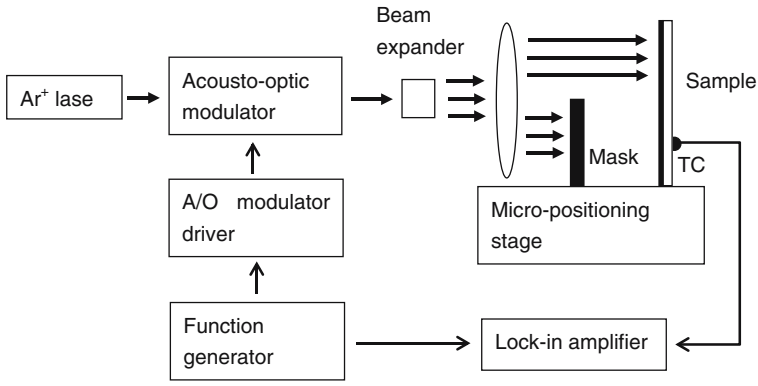

Fig. 2. Schematic diagram of the experimental setup for the ac calorimetric method.

amount of silver paste. Note that the thermocouple can be attached to the lower surface of the sample as the temperature field is one-dimensional. Since the thermal penetration depth is much smaller than the width of the sample, the temperature field can be assumed as one-dimensional. Furthermore, it can be shown that the presence of the thermocouple tip does not affect the result of the thermal diffusivity determination [12]. The output signals from the thermocouple are pre-amplified and fed to the lock-in amplifier. An optical mask installed on the micro-stage adjusts the distance from the light source to the thermocouple. The positioning system is controlled by a pc with a resolution of 1.25μm. The size of the thin-film sample is $5 \times 10\,\text{mm}^2$ and all the measurements are conducted at a temperature of 20°C.

The same experimental setup is used for thermal-diffusivity determination by the photothermal mirage technique, except for the temperature detection part. For optical temperature detection, the deflection of a HeNe laser beam (power of 4 mW, wavelength of 632.8μm) is monitored by a position sensitive photodetector. Details of the experimental setup for photothermal mirage measurements can be found in our previous work [11].

3. PREPARATION OF THIN FILM SAMPLES

The thin-film samples are fabricated by standard processes employed in typical MEMS applications. In the thermal diffusivity measurement of metallic thin films, the relative heat conduction through the film, i.e.,$d_f\sqrt{k_f C_f}/d_s\sqrt{k_s C_s}$, is a critical parameter that needs to be maximized. Consequently, all the thin-film samples are specially deposited on 25μm-thick polyimide substrates (Dupont, Inc. Kapton 100HN) to minimize the heat loss. The thermal effusivity ratio based on the measurement results is 5.2 – 12.8. The Au film of 1000 nm in thickness is deposited by the e-beam evaporation process with an Ar flow at 35 sscm. The pressure in the deposition chamber is kept at 0.53 Pa. The $Al_{0.97}Ti_{0.03}$ (400 nm), Sn (2000 nm), and Mo (350 nm) films are all deposited by the dc magnetron sputtering method at room temperature with dc power levels of 1000, 150, and 500 W, respectively. Ar gas flow was provided during the sputtering process, with flow rates of 40 – 50 sccm, depending on the sample. The chamber pressure was maintained at 0.4 Pa.

4. RESULTS AND DISCUSSIONS

Figure 3 displays the experimental raw data from the ac calorimetric measurement for the Au/polyimide sample. Measurements were first

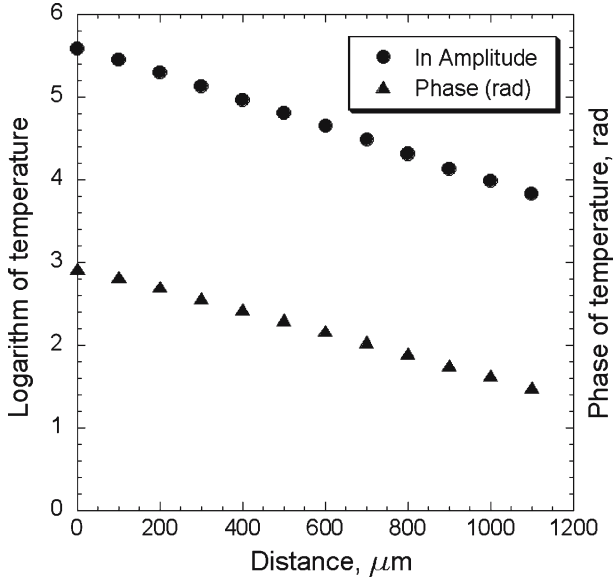

Fig. 3. Typical temperature signal obtained in the ac calorimetric method (Au, 1000 nm).

performed for Au as a reference case to ensure the accuracy of the experimental setup. The slopes of the two curves, one from the logarithm of the amplitude and the other from the phase, are 1.60 and 1.30 mm^{-1}, respectively, which indicates that the heat loss into the ambient air affects the measurement accuracy significantly. Accordingly, Eqs. (2) and (3) were used in this work to compensate for the effect of heat loss. Measurements were repeated eight times, and the results were averaged to determine the thermal diffusivity. The maximum and standard deviations of the measured data were 5.2% and 2.0%, respectively. The uncertainty considering the sample fabrication process was found to be 3.4% based on four different Au thin-film samples, indicating that the sample quality is sufficiently uniform to neglect the random error from the sample-to-sample variation. As the Au thin film generally has a good crystalline structure and the electron mean free path is only of the order of 10 nm [13], the thermal diffusivity of the 1000 nm thin film should be close to that of the bulk sample unless impurity scattering is significant. The measured thermal diffusivity of the Au thin film is 117×10^{-6} $m^2 \cdot s^{-1}$, which is lower by 7% than the bulk value of 127×10^{-6} $m^2 \cdot s^{-1}$ [14]. This result is also in good agreement with a literature value of 124×10^{-6} $m^2 \cdot s^{-1}$ for a 340 nm thick Au film prepared by a similar fabrication process [15].

In addition to the measurement by ac calorimetry, experiments were also conducted by employing the photothermal mirage technique as an alternative non-contact method. The results indicate that the random error is substantially greater than that of the ac calorimetric method. For example, the standard deviation of the repeated thermal diffusivity measurements is as large as 20.0%. It is believed that this increased random error is mainly due to the non-contact nature of the technique, i.e., difficulty in precise optical alignment and the influence of ambient air flow. Furthermore, the thermal diffusivities of the metallic thin films measured by the mirage technique were 25 – 37% smaller than those by ac calorimetry. For example, the measured thermal diffusivity of the Au film is 88×10^{-6} $m^2 \cdot s^{-1}$. Error analysis reveals that this bias of the measured data is mainly influenced by the effect of the sample temperature increase during the measurement. In the present experimental setup, relatively high-power laser irradiation of more than 500 mW was required to optically detect the thermal wave effectively, which resulted in considerable temperature increase. For instance, the maximum temperature rise at the center of the heating beam is estimated to be as large as 700°C for the case of Au (laser power of 0.5 W, frequency of 10 Hz). Since a surface temperature increase of 500 K can lead to a thermal conductivity drop of 15% [14], it can be claimed that the temperature increase is the main source of the bias error. On the other hand, the temperature increase measured by the thermocouple was less than 10°C for the case of the ac calorimetric method. Consequently, the results by the ac calorimetric method were used to quantify the thermal diffusivity of the thin films in the present study. Nevertheless, this work demonstrates that the mirage technique, as a non-contact method that does not require a sample preparation process, is effective for measuring the thermal diffusivity of thin films. It is also noted that the uncertainty of the mirage technique can be significantly reduced by decreasing the heat source power with an improved optical system and/or by adopting a controlled-gas cell as demonstrated in previous studies for example, Ref. [8]).

The thermal diffusivities as measured by the ac calorimetric method are listed in Table I with comparisons with bulk state results. Table I confirms that the thin-film thermal diffusivity is generally smaller than that of the same material in bulk form. The thermal diffusivity normalized by the corresponding bulk value varies from 0.513 to 0.986. It is noted that the normalized thermal diffusivity of the Al/Ti alloy thin film could not be calculated as the thermal diffusivity of bulk Al/Ti is unknown. Therefore, the normalized thermal diffusivity of the Al/Ti alloy in Table I is based on pure Al. It is obvious that impurity scattering by Ti atoms lowers the thermal diffusivity of the alloy significantly.

Table I. Experimental Results by the ac Calorimetric Method

Material	Thickness (nm)	Thin-film Thermal Diffusivity ($10^{-6}\,m^2\cdot s^{-1}$)	Bulk-material Thermal Diffusivity [14] ($10^{-6}\,m^2\cdot s^{-1}$)	Normalized Thermal Diffusivity
Au	1000	117	127	0.926
$Al_{0.97}Ti_{0.03}$	400	49.8	(97.1, pure Al)	(0.513, based on bulk Al)
Sn	2000	39.0	40.1	0.972
Mo	350	53.0	53.7	0.986

The electrical conductivity σ of the metal films was measured by the standard four-probe technique and the results are exhibited in Fig. 4. In the figure, the electrical conductivity is normalized by that of the same material in bulk form and compared with the normalized thermal conductivity. The normalized thermal conductivity has been calculated using bulk values of density and heat capacity. It is also noted that the thermal conductivity of the Al/Ti alloy is normalized by the thermal conductivity of pure Al in the bulk state. Figure 4 shows that the Mo thin film has an anomaly in the reduction of thermal/electrical conductivity from the bulk value. In Fig. 5, the Lorentz numbers, i.e., $L \equiv k/(\sigma T)$, are displayed for the thin films. It is shown that the electrical-conductivity drop is considerably larger than the thermal-conductivity drop for the case of the $Al_{0.97}Ti_{0.03}$ alloy and Mo thin films while the Lorentz number for Au and Sn is close to the theoretical prediction by the Sommerfeld theory of metals, i.e., $L = 2.44 \times 10^{-8}\,W\cdot\Omega\cdot K^{-2}$. The discrepancy in the Al/Ti alloy may be explained in terms of impurity scattering by the Ti atoms. However, other mechanisms such as boundary scattering may also be responsible for the phenomena. There is evidence that the presence of interface boundaries may affect thermophysical properties even in much thicker films than those examined in this work [16]. Since the scattering decreases the mean free path of the electrons, heat diffusion by phonons becomes relatively important and leads to deviations from the Wiedemann–Franz law. The thermal- and electrical-conductivity data reported in Ref. [6] also show similar deviations from the Wiedemann-Franz law.

The thin–film structures have been analyzed by XRD (X-ray diffraction) and AFM (atomic force microscope) analysis. The results are summarized in Figs. 6 and 7. The intensity peaks in Fig. 6 demonstrates that all the thin films are crystalline. The AFM images for Au, $Al_{0.97}Ti_{0.03}$, and Sn thin films in Fig. 7 shows clear grain boundaries in the size range

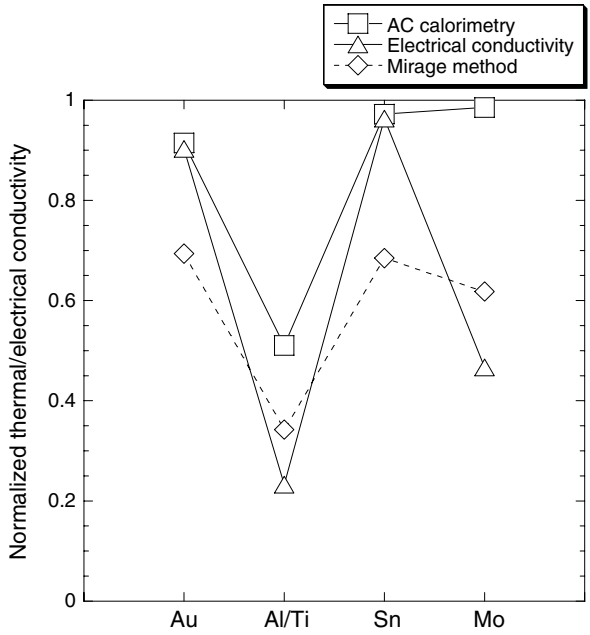

Fig. 4. Thermal and electrical conductivities normalized by the corresponding bulk properties.

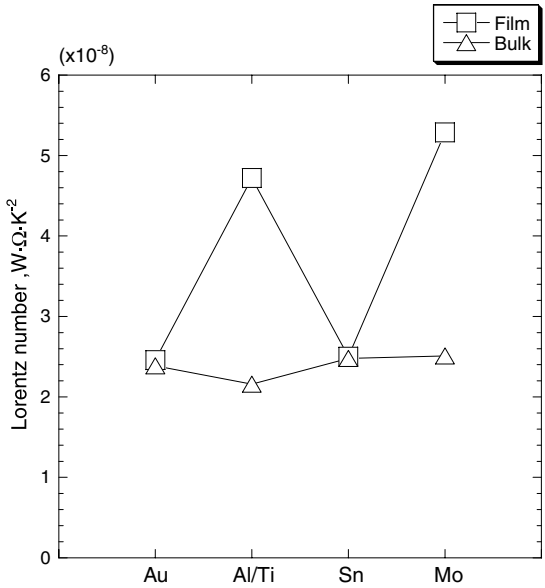

Fig. 5. Lorentz number of the metallic thin films.

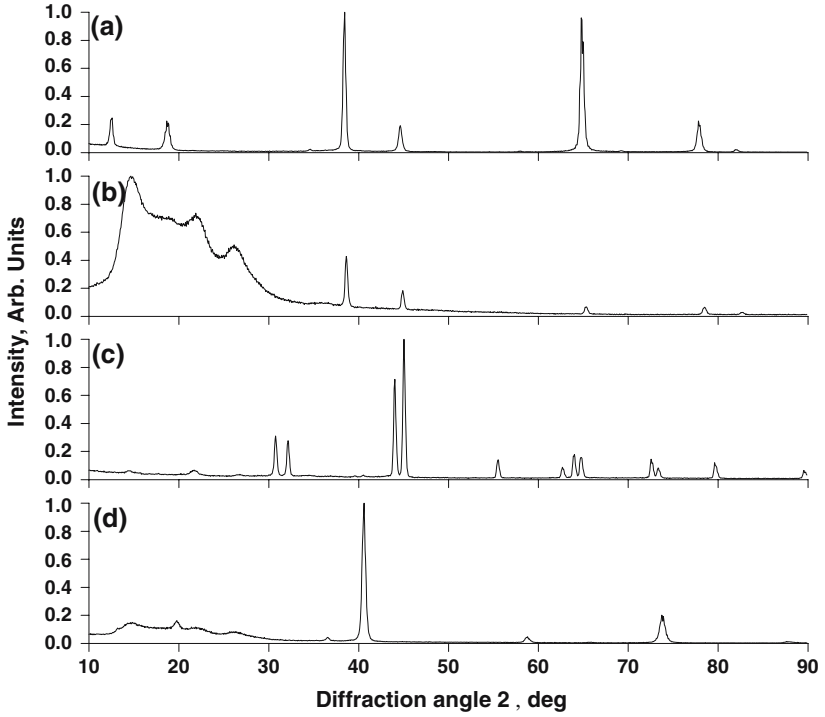

Fig. 6. X-ray diffraction patterns for (a) Au, (b) $Al_{0.97}Ti_{0.03}$, (c) Sn, and (d) Mo thin films.

of 200 – 2000 nm. These observations support the finding from the XRD analysis that the thin films have crystalline structures. However, the grain boundaries were less clear for the case of Mo, independent of the AFM magnification. A typical surface image of a Mo thin film sample is given in Fig. 7 d. Considering that the electron mean free path is generally tens of nanometers, the results of the structural analysis are consistent with the fact that the thermal conductivity reduction by the thin-film size effect is not significant for these materials. Accordingly, it can be claimed that the substantial reduction of the $Al_{0.97}Ti_{0.03}$ thermal conductivity is attributed mainly to the impurity scattering of Ti atoms. Also, these results are consistent with the fact that the Lorentz number of the $Al_{0.97}Ti_{0.03}$ thin film is higher than the theoretical prediction because the phonon mean free path is comparable to the electron mean free path. The observation that the relative electrical conductivity of the Mo thin film is much smaller than the relative thermal conductivity as displayed in Fig. 5 indicates that

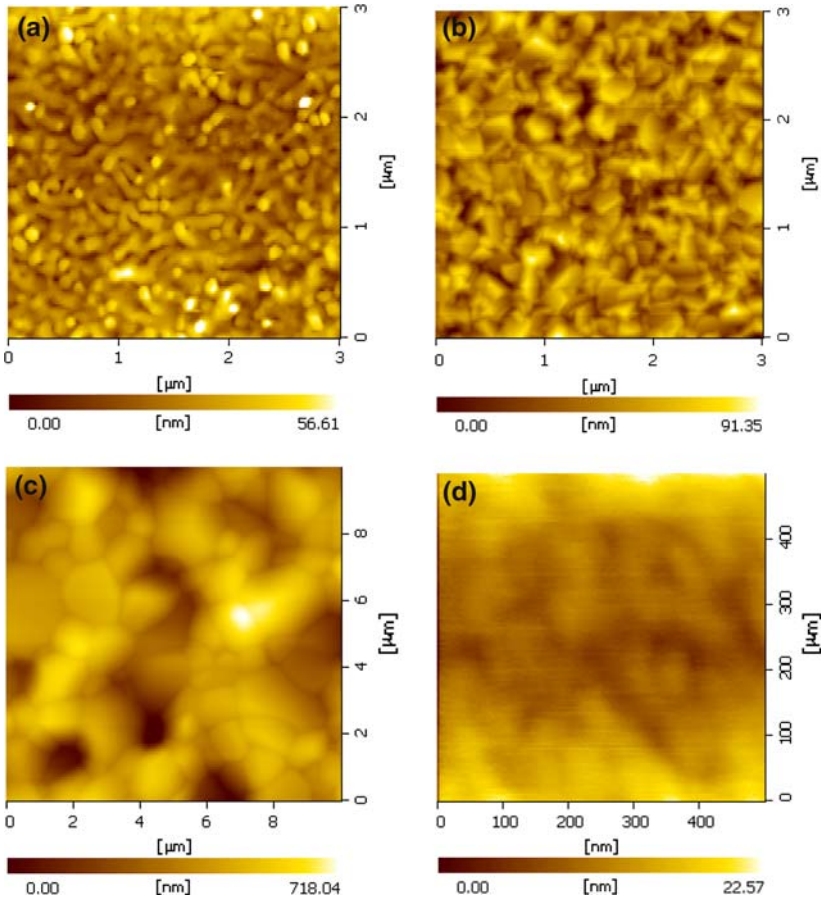

Fig. 7. AFM images of the thin-film surfaces for (a) Au, (b) $Al_{0.97}Ti_{0.03}$, (c) Sn, and (d) Mo thin films.

phonons play a significant role in heat diffusion in the thin film. However, the source of the anomaly for Mo is not clearly identified by the XRD and AFM analysis. Further investigations for delineating the detailed microstructures of the Mo thin film are therefore required for elucidating the thermal behavior of the film.

5. CONCLUSIONS

In this work, the thermal diffusivity of several metallic thin films deposited on polyimide substrates was measured for the first time by

the ac calorimetric method. Experiments using the photothermal mirage technique demonstrate that the non-contact technique can also be used to measure the thermal diffusivity of thin films effectively, validating the results of the ac calorimetric measurement. The measured thermal diffusivity of the thin film is smaller than that of the same material in the bulk state. Particularly, the $Al_{0.97}Ti_{0.03}$ alloy thin film exhibits a pronounced reduction of thermal diffusivity compared with bulk Al, which is believed to result from impurity scattering. The relation of thermal and electrical conductivities follows the Wiedemann–Franz law for the case of Au and Sn thin films. However, significant deviations from the theoretical prediction were observed for the $Al_{0.97}Ti_{0.03}$ alloy and Mo thin films.

ACKNOWLEDGMENTS

Support for this work is greatly appreciated: Micro Thermal System ERC, Grant for Advanced Laser Microfabrication, and KOSEF Basic Research Program.

REFERENCES

1. K. E. Goodson and Y. Sungtaek Yu, *Ann. Rev. Mater. Sci.* **29**:261 (1999).
2. D. G. Cahill, *Rev. Sci. Instrum.* **61**:802 (1990).
3. M. Asheghi, M. N. Touzelbaev, K. E. Goodson, Y. K. Leung, and S. S. Wong, *J. Heat Transfer* **120**:31 (1998).
4. H. K. Park, C. P. Grigoropoulos, and A. C. Tam, *Int. J. Thermophys*. **16**:973 (1995).
5. R. Kato, A. Maesono, M. P. Tye, and I. Hatta, *Int. J. Thermophys*. **20**:977 (1999).
6. N. Taketoshi, T. Baba, and A. Ono, *Meas. Sci. Technol.* **12**:2064 (2001).
7. Y. Gu, X. Tang, Y. Xu, and I. Hatta, *Jpn. J. Appl. Phys. B* **32**:L1365 (1993).
8. A. Mandelis, *Diffusion-Wave Fields* (Springer-Verlag, New York, 2001), p. 225.
9. J. Rantala, L. Wei, P. K. Kuo, J. Jaarinen, M. Luukkala, and R. L. Thomas, *J. Appl. Phys.* **73**:2714 (1993).
10. A. Salazar, A. Sánchez-Lavega, and J. Fernández, *J. Appl. Phys.* **65**:4150 (1989).
11. S. R. Choi and D. Kim, *Int. Symp. Micro/nanoscale Energy Conversion and Transport* (Seoul, 2004), pp. 91–93.
12. I. Hatta and T. Yamane, *Jpn. J. Appl. Phys.* **40**:393 (2001).
13. G. Chen, D. Borca-Tasuica, and R. G. Yang, *Nanoscale Heat Transfer*, in *Encyclopedia of Nanoscience and Nanotechnology*, Vol. 7, H. S. Nalwa, ed. (American Scientific Publishers, Stevenson Ranch, California, 2004), pp. 429–459.
14. J. F. Shackelford and W. Alexander, *CRC Materials Science and Engineering Handbook, 3rd Ed*. (CRC Press, Boca Raton, Florida, 2001).
15. T. Yamane, Y. Mori, S. Katayama, and M. Todoki, *J. Appl. Phys*. **82**:1153 (1997).
16. Y. Liu, A. Mandelis, M. Choy, C. Wang, and L. Segal, *Rev. Sci. Instrum*. **76**:084902 (2005).